

Nonlocal dc electrical conductivity of a Lorentz plasma in a stochastic magnetic field

Abram R. Jacobson and Ronald W. Moses

Los Alamos National Laboratory, Los Alamos, New Mexico 87545

(Received 12 December 1983)

The stochastic wandering of magnetic field lines allows momentum of even perfectly magnetized electrons to be transported across the mean \vec{B} . We include this effect, along with the usual acceleration and scattering terms, in a spatially one-dimensional Boltzmann equation for the electron distribution function. For an electric field $E_{||}$ (along local \vec{B}) which varies versus position normal to \vec{B} , the momentum transport leads to a nonlocal electrical conductivity. We apply the formalism to sheared, force-free magnetoplasmas, in which the $E_{||}$ gradient is caused by variable twisting of \vec{B} with respect to an externally applied uniform \vec{E} . We examine in particular the experimentally documented phenomenon of field-aligned current density $j_{||} > 0$ in regions of the sheared magnetic field where $E_{||} \approx 0$ or even $E_{||} < 0$. This phenomenon is in apparent violation of Ohm's law. Under suitable conditions of stochasticity and collisionality, we find that the spatial structure and temporal persistence of these force-free configurations can be directly caused by electron-momentum transport. This result is derived solely on the basis of electron dynamics. In contrast to fluid-turbulent models, our kinetic derivation requires no hypothetical "plasma dynamo" and no conjecture on the decay rates of magnetic helicity versus magnetic energy.

I. INTRODUCTION

The notion of electrical conductivity is based on a local constitutive relation between electric field \vec{E} and current density \vec{j} . The local Ohm's law implies a pointwise balance momentum gain (via \vec{E}) and momentum loss (via scattering) on the part of the charge carriers. The local Ohm's law for plasma¹ is regularly used in calculations of plasma dynamics, transport, and equilibrium. In contrast, if momentum gain and momentum loss are only globally, but not locally, in balance, then we must develop a nonlocal conductivity.

Consider field-aligned currents carried by a plasma embedded in an equilibrium uniform-magnitude magnetic field \vec{B}_0 . At $x=0$, $\vec{B}_0(0)=\hat{z}B_0$. At locations $x > 0$, the magnetic field becomes rotated by an angle ϕ , so that $\vec{B}_0(x)=B_0(\hat{z}\cos\phi+\hat{y}\sin\phi)$. The rotation ("magnetic shear") is caused by field-aligned current density $j_{||}(x)$. Let the currents be driven by a uniform electric field $\vec{E}=E_z\hat{z}$. Then the component of \vec{E} along \vec{B} is $E_{||}(x)=E_zB_z(x)/B_0$, which varies with x . The gradient $\partial E_{||}/\partial x$ would cause nonlocal-conductivity effects—whatever their origin—to have significant effects on the magnetic equilibrium.

We base our nonlocal-conductivity model on the motions of electrons in a magnetic field which is subject to many small, spatially overlapping perturbations. The magnetic perturbations \vec{B}_1 include B_{1x} components. Provided that the perturbations cause overlap of magnetic island structures, the magnetic flux surfaces are then destroyed.² Instead of remaining confined within its y - z plane, a magnetic field line will now wander randomly in x . The mean-square displacement in x accrued during a

path length l may then be approximated as if it wandered ergodically:

$$\langle(\Delta x)^2\rangle=2lD_F, \tag{1}$$

where D_F is the field-line diffusivity.² Rechester and Rosenbluth³ have shown how the diffusion of electrons in such a magnetic field system leads to enhanced "cross-field" heat transport. In this paper we discuss the analogous process of electron-momentum transport. We define $\langle(\Delta x)^2\rangle_p$ as the mean-square, cross- \vec{B}_0 excursion of an electron in one mean free path (for cumulative scattering through 90°) as it wanders along a stochastic field line [see Eq. (1)]. We then define a locality parameter α ,

$$\alpha=\langle(\Delta x)^2\rangle_p\left[\frac{1}{E_{||}}\frac{\partial E_{||}}{\partial x}\right]^2. \tag{2}$$

For $\alpha \ll 1$ a local Ohm's law is correct. However, for $\alpha \gtrsim 1$ the cross-field momentum transport causes electron scattering to occur far (in x) from the locality of acceleration. The assumption of pointwise balance between momentum gain and momentum loss is no longer true, and the local Ohm's law must be replaced by a global solution over the entire $E_{||}$ gradient.

We will assume that the magnitude B_0 of the magnetic field is uniform, and that the electron's pitch angle is adiabatically conserved during the electron's field-aligned wander, *except for collisions*. That is, the field-line wander is due to sufficiently gentle local-field-line curvatures that the electron's magnetic moment is not affected by the curvatures. Furthermore, we shall ignore effects of finite electron Larmor radius or of electron drifts perpendicular to \vec{B} .

In Sec. II we shall derive the differential equation for the perturbed electron distribution function in the presence of stochastic magnetic fields. In order to characterize this new effect as clearly as possible, the simple Lorentz ion model will be used. The neglect of electron-electron scattering will, in a manner similar to its effect on local-conductivity results,¹ cause our crude model to overstate the overall current by a factor on the order of ~ 2 .

The second major simplification in our model of nonlocal conductivity will be to treat only a homogeneous (i.e., isothermal and isodense) background electron distribution function. This simplification allows us to avoid two technical complications in the analysis. First, if an electron temperature gradient $\partial T/\partial x$ or electron density gradient $\partial n/\partial x$ were present while electrons could sample the gradient length between collisions, it would no longer be possible to represent the local background distribution by a Maxwellian in local thermodynamic equilibrium. Instead, the background distribution function would be significantly distorted by thermal conduction even before the electric field's contribution is considered. Second, the Lorentz's model's neglect of electron-electron scattering would lead to serious errors if an electron could wander significantly along, for example, the $\partial T/\partial x$ gradients during one collision time. This is because the effective collision length λ would now be a function of x , in view of the x -dependent velocity spectrum of the background electrons. Such an effect is beyond the scope of our simple Lorentz model. For both of these reasons we confine our analysis to the case of uniform electron density and temperature.

The nonlocal-conductivity equation will then be solved for steady-state force-free magnetoplasmas in Sec. III. It has been customary to explain the observed persistence of certain of these configurations on the basis of hypothesized magnetofluid turbulence. However, we will show that under appropriate conditions of collisionality and stochasticity, the key structural and temporal properties of force-free magnetoplasmas may be explained entirely on the basis of electron-momentum diffusion.

II. INCLUSION OF MOMENTUM SPREADING IN THE PERTURBED DISTRIBUTION FUNCTION

A. Significance of collisionality

Consider a test electron carrying parallel momentum $p_{\parallel} = mv_{\parallel}$. Using the terminology of Ref. 3, we distinguish between "collisional" and "collisionless" electrons: The collisional electron's 90°-scattering length λ is short compared with the "correlation length" L_F of a field line.² (The field-line correlation length is, effectively, the correlation length of B_x computed along the wandering field-line's path.) For collisionless electrons, however, $\lambda \gg L_F$. The collisional electron will lose the sign of its parallel momentum during a single "straight" path within which B_x is essentially constant. The collisionless electron, on the other hand, will random-walk in x within a collision time, sampling many spatial phases of the B_x

perturbations. The particle diffusivity³ which results in the collisionless case is

$$D_e = D_F |v_{\parallel}|, \quad (3)$$

where v_{\parallel} is the velocity parallel to \vec{B} . Only the magnitude, not the sign, of v_{\parallel} affects the particle diffusion. This feature will be important in Sec. IIB. Within one collision time, the electron momentum also "diffuses" in the x direction. However, for times longer than a scattering time, the sign of the momentum is lost. Therefore Eq. (3) is not complete for momentum (although it does suffice for particle, or particle energy, or indeed any even power of \vec{v}_{\parallel}) diffusion. The diffusion term may be utilized in a Boltzmann equation which also includes Coulomb collisions; the solution will reflect a balance between scattering and diffusive spreading.

The conductivity calculation to follow assumes that the perturbation induced by E_{\parallel} may be described by a laminar perturbation $f^{(1)}(\vec{v}, x)$ in the electron distribution function. Thus we require $\partial f^{(1)}/\partial y, \partial f^{(1)}/\partial z \approx 0$. At first glance this would appear unlikely to be satisfied, because the magnetic perturbations are intrinsically *nonlaminar*: $|\hat{x} \times \vec{\nabla} B_x|$ is *not* small. However, there is a regime in which the distribution function $f^{(1)}(\vec{v}; x, y, z)$ may be approximated by a laminar $f^{(1)}(\vec{v}, x)$ despite the obviously nonlaminar properties of B_x . This can be seen by noting that an electron drifting along \vec{B} (with field-aligned velocity component v_{\parallel}) only "remembers" impulses (due to E_{\parallel}) which occurred within the immediately preceding mean free time. Equivalently, the electron remembers E_{\parallel} only along the mean free path λ it has just traversed. Here the concept of collisionality from Ref. 3 plays a crucial role. Consider a plane $x = x_0$ within a strong gradient $\partial E_{\parallel}/\partial x > 0$. If the electrons are collisional, then $f^{(1)}(\vec{v}; x_0, y, z)$ will have y and z variations closely replicating $B_x(x_0, y, z)$. This is because a collisional electron with, for example, $v_{\parallel} > 0$ arriving from $x < x_0$ (i.e., drifting in a region where $B_x > 0$) remembers only a weak E_{\parallel} , while one arriving from $x > x_0$ (i.e., in a region where $B_x < 0$) remembers only a strong E_{\parallel} . Electrons with $\lambda \gg L_F$, however, will cause $f^{(1)}(\vec{v}; x_0, y, z)$ to be much smoother than $B_x(x_0, y, z)$. This is because any region ($B_x > 0$ or $B_x < 0$) of the plane $x = x_0$ now contains electrons which remember impulses due to E_{\parallel} accrued over an ensemble of random walks in the gradient $\partial E_{\parallel}/\partial x$.

Therefore, the conductivity calculation (below) is restricted to the collisionless³ case: $\lambda \gg L_F$. The assumption of a laminar $f^{(1)}(\vec{v}, x)$ would be invalid for the collisional³ case.

B. Neglect of space-charge effects

The linearized (i.e., infinitesimal E_{\parallel}) solution to both the local conductivity¹ and to the nonlocal conductivity [see Eq. (11) below] have a feature in common: For any given v , the number-density perturbation $f^{(1)}(\vec{v}, x)$ is purely odd in $\cos\theta$ (where θ is the angle between \vec{v} and \vec{E}_{\parallel} which is aligned with \vec{B}). For a given v , the electron number density with $\theta = \theta_0$ is depleted (enhanced) by the same amount as the number density with $\theta = \theta_0 + 180^\circ$ is

enhanced (depleted). This means that although electron parallel momentum is transported down the gradient $\partial |E_{||}| / \partial x$ [see Eq. (3) and its discussion], net electron number density (averaged over θ) with speed v is *not* transported down the gradient. Thus we are justified in ignoring an E_x generated by space-charge accumulation; in the linear regime such accumulation does not occur.

Were one to consider nonlinear solutions, one would need to compute the perturbed total electron number density versus x and use Poisson's law to generate $E_x(x)$ from the space charge. The E_x would drive an electron return flux up the gradient $\partial |E_{||}| / \partial x$. The return flux would be made possible by the stochastic wandering (in x) of field lines. We have not investigated this return flux in detail because in the linear regime space charge does not accumulate. However, we remark that, on the basis of symmetry, the return flux driven by space charge E_x in the nonlinear regime will only carry electron charge, but *not electron parallel momentum*, back up the gradient.

C. Criterion for requiring nonlocal solution

In order to decide when a nonlocal conductivity is required, the mean-square displacement $\langle (\Delta x)^2 \rangle$ for momentum can be roughly estimated using Eq. (1) with a known D_F . The locality parameter should be evaluated using the electron mean free path averaged in a way that properly weights each electron velocity's importance in carrying current. We can then show the extreme importance of electrons in the tail of the background Maxwellian distribution. Thus l is taken as the 90° scattering length (ignoring θ dependence) averaged over the electron speed weighted by the differential current $dj/d(v/v_0)$. For a Lorentz plasma, the latter is¹

$$\frac{dj}{d(v/v_0)} \sim \left[\frac{v}{v_0} \right]^7 e^{-(v/v_0)^2}, \quad (4)$$

where $v_0 \equiv \sqrt{2kT/m}$ is the Maxwellian's most probable speed. The mean free path (considering scattering off fixed Lorentz ions) for speed v is written

$$\lambda_v = \lambda_0 \left[\frac{v}{v_0} \right]^4, \quad (5)$$

where $\lambda_0 \equiv 90^\circ$ scattering length for $v = v_0$ and $\cos\theta = 1$.

The averaged scattering length (ignoring θ dependence) is then

$$l_S = \frac{1}{j} \int_0^\infty \lambda_v \frac{dj}{dv} dv = 20\lambda_0. \quad (6)$$

The locality parameter [Eq. (2)] would then be written

$$\alpha = 40\lambda_0 D_F \left[\frac{1}{E_{||}} \frac{\partial E_{||}}{\partial x} \right]^2. \quad (7)$$

The result [Eq. (6)], that $l_S = 20\lambda_0$, reflects the importance of tail electrons ($v > v_0$) in carrying current. (In the exact solution¹ including electron-electron scattering, we would get $l_S \approx 5\lambda_0$.)

D. Boltzmann equation for nonlocal conductivity

Let $f^{(0)}(\vec{v})$ be a (spatially uniform) background Maxwellian distribution. Then the Boltzmann equation for the space-dependent perturbation $f^{(1)}(\vec{v}, \vec{r})$ would normally be written¹ (with \vec{a} identically equal to acceleration):

$$\frac{\partial f^{(1)}(\vec{v}, \vec{r})}{\partial t} + \vec{v} \cdot \vec{\nabla}_r f^{(1)}(\vec{v}, \vec{r}) + \vec{a} \cdot \vec{\nabla}_v f^{(1)}(\vec{v}, \vec{r}) = \frac{\partial f^{(1)}(\vec{v}, \vec{r})}{\partial t} \Bigg|_{\text{coll}}. \quad (8)$$

In principle, the Boltzmann equation [Eq. (8)] in this form could be subjected to certain averaging procedures which would lead to diffusion of electrons in the stochastic magnetic field. The important terms leading to such diffusion would be (a) the convective term $\vec{v} \cdot \vec{\nabla}_r f^{(1)}$ and (b) the Lorentz electromotance $\vec{v} \times \vec{B}$ contained in the term involving acceleration.

The development from Eq. (8) becomes far simpler, however, in our long-collision-length regime ($\lambda \gg L_F$), because we can exploit two approximations: First, the perturbed distribution function is laminar, varying only with x . Second, as shown by Rechester and Rosenbluth,³ the effect of a gradient $\partial f^{(1)}/\partial x$ will be to drive a diffusive flux $-D_e \partial f^{(1)}/\partial x$ down the gradient as in a Fick's law. The divergence of that flux is (minus) the time rate of change of $f^{(1)}$ due to the diffusive flux. This leads to a scatteringlike term

$$\frac{\partial f^{(1)}(\vec{v}, x)}{\partial t} \Bigg|_{\text{diff}} = |v_{||}| \frac{\partial}{\partial x} \left[D_F(x) \frac{\partial f^{(1)}(\vec{v}, x)}{\partial x} \right]. \quad (9)$$

The Boltzmann equation with the above approximations then becomes

$$\frac{\partial f^{(1)}(\vec{v}, x)}{\partial t} - \frac{e}{m} E_{||}(x) \frac{\partial f^{(0)}(\vec{v})}{\partial v_{||}} = \frac{\partial f^{(1)}(\vec{v}, x)}{\partial t} \Bigg|_{\text{coll}} + \frac{\partial f^{(1)}(\vec{v}, x)}{\partial t} \Bigg|_{\text{diff}}. \quad (10)$$

The diffusive term expresses the rate of influx of electrons (with velocity between \vec{v} and $\vec{v} + d\vec{v}$, into the zone between x and $x + dx$) as if collisions did not take place. The collisions are handled, however, in the normal manner, by the first term on the right-hand side of Eq. (10). The two effects are assumed to be superimposable.

In steady state Eq. (10) becomes

$$f^{(1)}(\vec{v}, x) = \frac{-E_{||}(x)}{E_c} \left[\frac{v}{v_0} \right]^4 \cos\theta f^{(0)}(\vec{v}) + 2\lambda_0 \left[\frac{v}{v_0} \right]^4 |\cos\theta| \frac{\partial}{\partial x} \left[D_F(x) \frac{\partial f^{(1)}(\vec{v}, x)}{\partial x} \right], \quad (11)$$

where E_c is the critical electric field.⁴ The first term on the right-hand side of Eq. (11) is the local solution.¹ The

second term is the modification for diffusive spreading of electron momentum.

E. Electrical current density and current-density transport

The distribution function obtained by solving Eq. (11) may be integrated over velocity (with $-ev_{\parallel}$ weighting) to give the current density parallel to \vec{B} :

$$j_{\parallel}(x) = -e \int v \cos\theta f^{(1)}(\vec{v}, x) d\vec{v}. \quad (12)$$

(Here the integration is over 4π steradians and $0 \leq v \leq \infty$.)

The nonlocal-conductivity effect relies on transport of field-aligned electron momentum down the gradient $\partial |E_{\parallel}| / \partial x$. The electron shear stress associated with this process is

$$\Gamma_{px}(x) = -mD_F(x) \int v^2 \cos\theta |\cos\theta| \frac{\partial f^{(1)}(\vec{v}, x)}{\partial x} d\vec{v}. \quad (13)$$

The shear stress Γ_{px} is the field-aligned electron momentum transported sideways across unit area (of a plane $x = \text{const}$) per unit time. Closely related is the current transport Γ_{jx} defined as the field-aligned current transported sideways across unit area (of a plane $x = \text{const}$) per unit time:

$$\Gamma_{jx} = -\frac{e}{m} \Gamma_{px}. \quad (14)$$

The current transport Γ_{jx} is responsible for distributing the current density j_{\parallel} more evenly (versus x) than a local solution [$j_{\text{loc}}(x) = \sigma E_{\parallel}(x)$]. It is the current transport which forces us to abandon a local Ohm's law in certain regimes of collisionality and stochasticity.

III. STRUCTURE AND PERSISTENCE OF HIGHLY SHEARED FORCE-FREE MAGNETOPLASMAS WITH STOCHASTIC MAGNETIC FIELDS

A. Background

The phenomenon of a plasma current whose force-free self-magnetic field is comparable to (or larger than) the background potential field is known to occur in astronomical plasmas (e.g., solar coronal loops⁵) and has been extensively exploited in laboratory plasmas [e.g., the reversed-field pinch⁶ (RFP) and spheromak⁷ classes of experiments]. Common features of these latter plasmas are as follows.

(1) Force-free (i.e., field-aligned) currents dominate; frequently $\vec{j} \times \vec{B}$ can be neglected.

(2) The magnetic field is highly sheared, rotating by 90° (as in a spheromak) or even more (as in an RFP).

(3) The ratio $\mu \equiv j_{\parallel}/B$ of the field-aligned current density to the field intensity tends toward a spatial constant.⁶

Furthermore, the RFP (e.g., the ZT-40 experiment⁷) discharge has been observed in certain regimes to persist far longer than is apparently allowed by resistive diffusion of the magnetic field.⁸ Specifically, the force-free currents at all angles to the applied electric field $\vec{E}_{\text{ext}} = \hat{z}E_z$ are observed to persist on a quasisteady time scale⁸ as though

$E_{\parallel}(r) = j_{\parallel}(r)/\sigma_{\parallel}(r)$ were satisfied, which it is not.

It has been hypothesized elsewhere that both the μ profile and the quasisteady persistence of RFP discharges could be due to a turbulent "dynamo" process.^{9,10} The dynamo would supply both fluctuating velocity \vec{v}_1 and fluctuating magnetic field \vec{B}_1 in correct magnitude and relative phasing to create a time-averaged electromotance $\langle \vec{v}_1 \times \vec{B}_1 \rangle$ which reconciles Ohm's law, viz.,

$$j_{\parallel} = \sigma_{\parallel} [E_{\parallel} + \langle (\vec{v}_1 \times \vec{B}_1)_{\parallel} \rangle]. \quad (15)$$

The plasma-dynamo hypothesis has never been confirmed in laboratory plasmas by joint measurements of velocity and magnetic field fluctuations. Nor has any self-consistent fluid-dynamical calculation of a dynamo shown the quasilaminar, axisymmetric, and quiescent properties observed in certain RFP experiments.^{6,7}

B. Slab-model force-free states with uniform magnetic diffusivity

We consider a bounded plasma between $x = \pm a$ with $j_{\parallel}(x)$ having even symmetry in x . The magnetic field diffusivity D_F is uniform within this region. The boundaries ($x = \pm a$) are considered insulating; that is, the electron-momentum stress is required to vanish at $x = \pm a$. Physically, this could represent, e.g., the onset of good (nonstochastic) flux surfaces for $|x| > a$. The boundary conditions of $f^{(1)}(\vec{v}, x)$ are then

$$\left. \frac{\partial f^{(1)}(\vec{v}, x)}{\partial x} \right|_{x=0} = \left. \frac{\partial f^{(1)}(\vec{v}, x)}{\partial x} \right|_{x=a} = 0. \quad (16)$$

We then solve the Boltzmann equation [Eq. (11)] for each of 39 velocities (3 angles times 13 speeds). The solutions at any x are tabulated and integrated with splines to obtain the current density [Eq. (12)] and the current-density transport [Eq. (13)]. The solution of Eq. (11) is necessarily iterative because the driving electric field $E_{\parallel}(x)$ varies due to the magnetic shear, viz.,

$$\frac{E_{\parallel}(x)}{E_z} = \frac{B_z(x)}{B}. \quad (17)$$

The force-free magnetic shear, in turn, obeys Ampere's law with $\vec{j} \times \vec{B} = \vec{0}$, viz.,

$$\frac{\partial B_y}{\partial x} = \mu \alpha j_{\parallel} \frac{B_z}{B}, \quad (18a)$$

$$\frac{\partial B_z}{\partial x} = -\mu \alpha j_{\parallel} \frac{B_y}{B}. \quad (18b)$$

Thus the iterative solution of Eq. (11) proceeds as follows.

- (1) A trial solution $E_{\parallel}(x)$ is chosen.
- (2) The Boltzmann equation is solved for $f^{(1)}(\vec{v}, x)$ at each of 39 velocities.
- (3) The current density $j_{\parallel}(x)$ is computed [Eq. (12)].
- (4) The profile B_z/B is computed from the j_{\parallel} profile [Eq. (18)].
- (5) A new E_{\parallel}/E_z profile is obtained [by Eq. (17)]; then return to (2).

Each convergent solution obtained from this iteration is tagged by two independent dimensionless parameters.

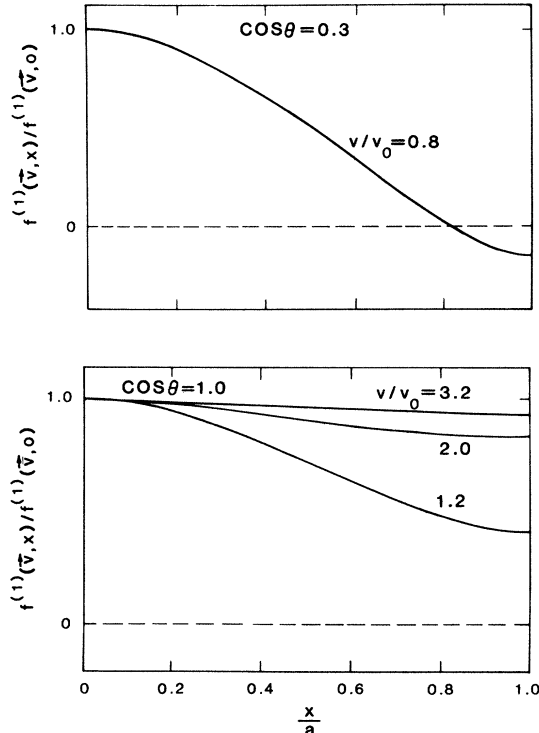


FIG. 1. Perturbation $f^{(1)}(\vec{v}, x)$ vs x for various \vec{v}' s, with $\lambda_0 D_F/a^2 = 0.05$. Each curve is normalized by $f^{(1)}(\vec{v}, 0)$. Top: $\cos\theta = 0.3$. Bottom: $\cos\theta = 1.0$.

The first is $a\mu_0 j_{||}(0)/B$, which serves as a starting wave number in Ampere's law. The second is $\lambda_0 D_F/a^2$, which measures the importance of momentum diffusion [see Eq. (11)].

Figure 1 shows the shape of solutions $f^{(1)}(\vec{v}, x)$ for individual velocities, with $\lambda_0 D_F/a^2 = 0.05$ and $a\mu_0 j_{||}(0)/B = 2.2$. The case illustrated in the top panel ($\cos\theta = 0.3$; $v/v_0 = 0.8$) almost tracks the applied $E_{||}(x)$ shape (see Fig. 2), because the low speed (hence short mean free time) and mainly cross-field orientation both disfavor nonlocal effects. The field-aligned orientations (Fig. 1, bottom panel) at higher speeds, in contrast, show the systematic trend toward more spatially uniform solutions.

The magnetic field and force-free current profiles for this case are shown in Fig. 2. The $j_{||}(x)$ profile has been

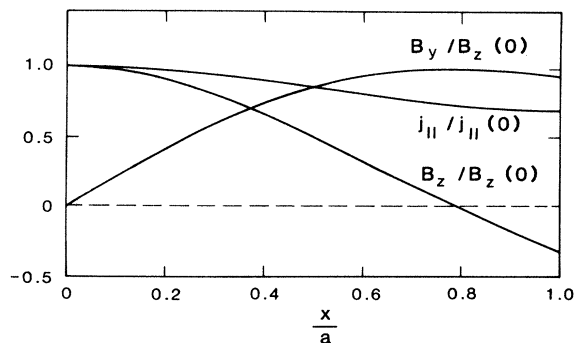


FIG. 2. Magnetic field components and parallel current density vs x , with $\lambda_0 D_F/a^2 = 0.05$. Each curve is normalized to 1 at $x = 0$.

normalized to its peak value at $x = 0$. The nominal local Ohm's-law current density is $\sigma_L E_z$ (where σ_L is the conductivity using the Lorentz model). The ratio $j_{||}(0)/(\sigma_L E_z)$ is actually 0.505. This ratio is less than unity because of electron-momentum transport. The axial field profile B_z/B is effectively the $E_{||}$ profile [see Eq. (17)].

The $j_{||}$ profile in Fig. 2 has a much flatter shape than does the B_z/B (and hence $E_{||}$) profile, as a result of electron-momentum transport. The current extends all the way to the insulating surface ($x = a$), and $\partial j_{||}/\partial x$ vanishes there. In the edge region $j_{||} > 0$, but $E_{||} < 0$.

The current-density transport [Eq. (14)] has units of (current/area) time $^{-1}$. We normalize using a/v_0 as a time and using the nominal local Ohm's law current density $\sigma_L E_z$. The normalized transport (for the same conditions as Figs. 1 and 2) is shown in Fig. 3. The gradient $\partial \Gamma_{jx}/\partial x$ is proportional to the rate at which electron momentum is being locally removed. At the profile's peak, scattering and acceleration are in exact balance. To the left of the peak, acceleration exceeds scattering, and momentum is being exported. To the right of the peak, scattering exceeds acceleration, and momentum is being imported.

We now adopt the ratio $B_y(a)/\langle B_z \rangle$ (where $\langle B_z \rangle$ is identically equal to x -averaged B_z) as a dimensionless parameter to replace $a\mu_0 j_{||}(0)/B$, in order to facilitate comparisons with the phenomenology of force-free configurations.⁶ [The value for the calculation in Figs. 1–3 was $B_y(a)/\langle B_z \rangle = 2.10$.] Figure 4 shows the peak normalized [using $j_{||}(0)$, not $\sigma_L E_z$, as the scale current] current-density transport as a function of $B_y(a)/\langle B_z \rangle$, for various diffusivities. The top curve ($\lambda_0 D_F/a^2 = \infty$) is an analytic, sinusoidal solution ($j_{||} = \text{const}$ versus x), while the others are numerically calculated. [For the simple analytic case ($j_{||} = \text{const}$) we have $a\mu_0 j_{||}/B = B_y(a)/\langle B_z \rangle$.] The current transport goes up as $\lambda_0 D_F/a^2$ goes up, at constant $B_y(a)/\langle B_z \rangle$. This is because the range of electron wander between collisions increases at larger $\lambda_0 D_F/a^2$. The transport goes up as $B_y(a)/\langle B_z \rangle$ goes up, at constant $\lambda_0 D_F/a^2$. This is because the gradient length $E_{||}(\partial E_{||}/\partial x)^{-1}$ becomes shorter at higher values of axial current [see Eqs. (2), (17), and (18)]. As the gradient length decreases, current transport must increase to sus-

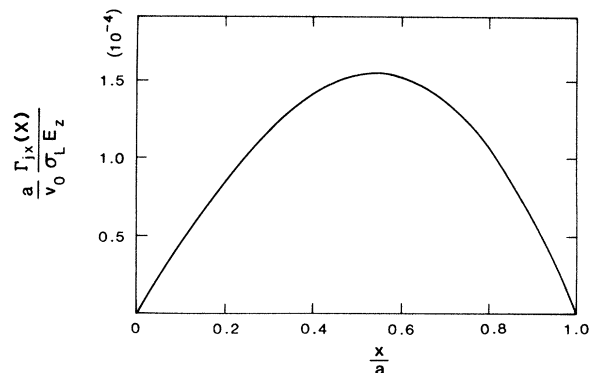


FIG. 3. Normalized current transport vs x , with $\lambda_0 D_F/a^2 = 0.05$. The scale current is $\sigma_L E_z$.

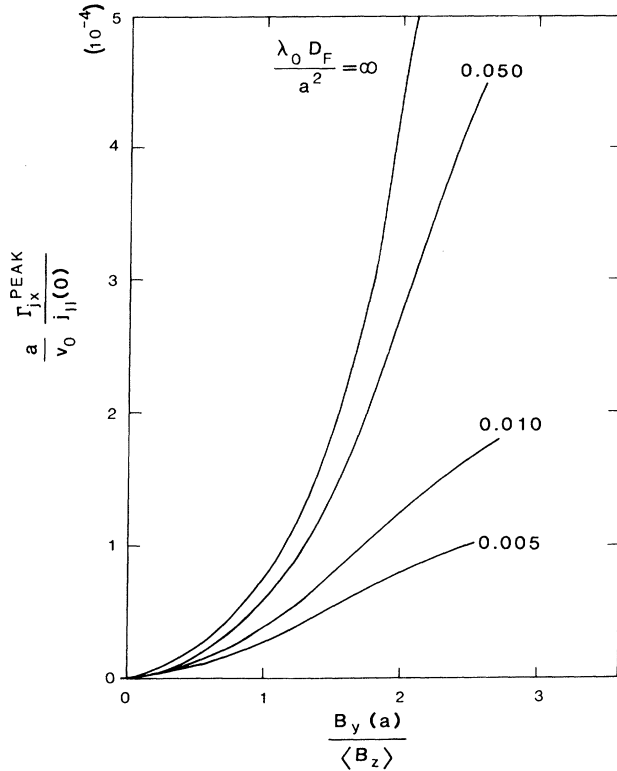


FIG. 4. Peak normalized current transport vs $B_y(a)/\langle B_z \rangle$, for various $\lambda_0 D_F/a^2$. The scale current is $j_{||}(0)$.

tain $j_{||}$ in regions of low or reversed $E_{||}$.

Figure 5 shows the ratio $\sigma_L E_z/j_{||}(0)$ vs $B_y(a)/\langle B_z \rangle$ for various diffusivities. This ratio measures the increase in applied electric field required to drive the peak current density $j_{||}(0)$. This ratio varies parametrically with $\lambda_0 D_F/a^2$ and with $B_y(a)/\langle B_z \rangle$ in the same manner as does the current-density transport, and for the same reasons.

The phenomenological descriptions^{6,9} of cylindrical force-free plasma configurations are often in terms of “ F - θ ” trajectories.⁶ The equivalent diagram for our slab problem is $B_z(a)/\langle B_z \rangle$ vs $B_y(a)/\langle B_z \rangle$, shown in Fig. 6 for various diffusivities. The lowermost curve ($\lambda_0 D_F/a^2 = \infty$) is the $j_{||} = \text{const}$ slab model solutions. [It is analogous to the cylindrical “relaxed state” ($j_{||}/B = \text{const}$) inferred by Taylor⁹ from the hypothesis that (with nonzero resistivity) magnetic helicity should decay more slowly than magnetic energy.] The curves with finite $\lambda_0 D_F/a^2$ exhibit shallower reversal [in the ordinate $B_z(a)/\langle B_z \rangle$] and a higher threshold [in the abscissa $B_y(a)/\langle B_z \rangle$] to achieve reversal. The limit $\lambda_0 D_F/a^2 = 0$ would approach $B_z(a)/\langle B_z \rangle = 0$ asymptotically but would never reverse. (This is analogous to the cylindrical force-free paramagnetic model.¹¹)

We may summarize the properties of these slab-model uniform-diffusivity force-free states.

(1) The key parameter governing electron-momentum diffusion and subsequent nonlocal effects is $\lambda_0 D_F/a^2$, the product of scattering length times magnetic diffusivity (in units of the system thickness).

(2) A secondary determinant of nonlocal effects’ impor-

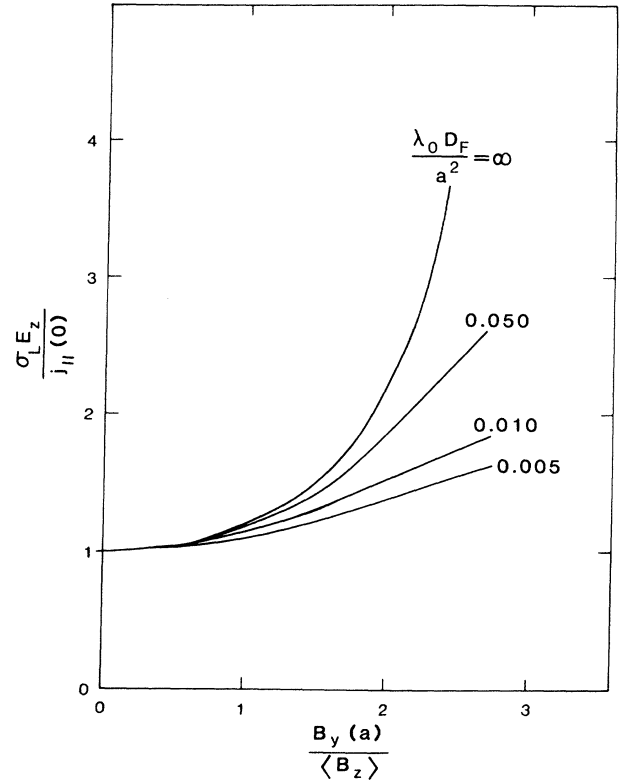


FIG. 5. Ratio of required electric field to that which would be expected [on the basis of a local Lorentz resistivity and the configuration’s $j_{||}(0)$] vs $B_y(a)/\langle B_z \rangle$, for various $\lambda_0 D_F/a^2$.

tance is the gradient length $E_{||}(\partial E_{||}/\partial x)^{-1}$; unlike $\lambda_0 D_F/a^2$, the gradient length is a function of the computed equilibrium itself.

(3) As nonlocal effects increase, the $j_{||}(x)$ profile tends to approach $j_{||} = \text{const}$.

(4) For finite values of $\lambda_0 D_F/a^2$, the current profile $j_{||}(x)$ has a behavior bounded by a fully “relaxed” state ($\lambda_0 D_F/a^2 \rightarrow \infty$) on the one hand, and a simple paramagnetic state ($\lambda_0 D_F/a^2 \rightarrow 0$) on the other.

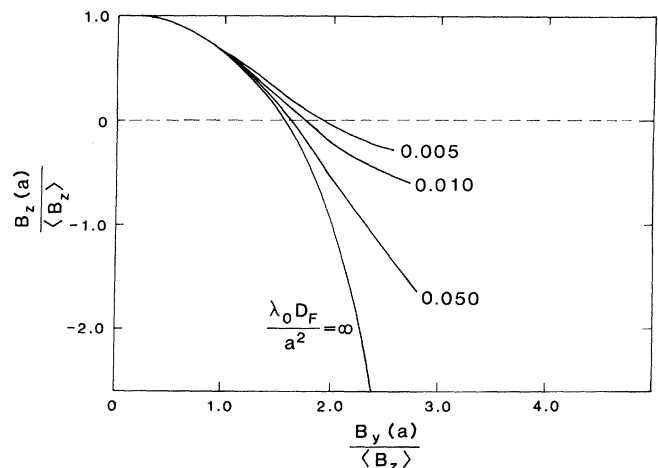


FIG. 6. $B_z(a)/\langle B_z \rangle$ vs $B_y(a)/\langle B_z \rangle$ for various $\lambda_0 D_F/a^2$.

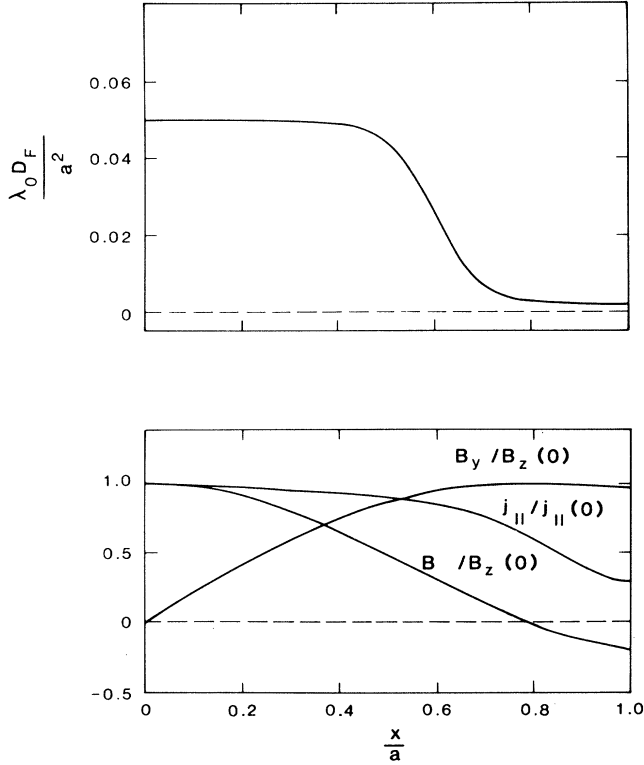


FIG. 7. Tapered-diffusivity model. Top: $\lambda_0 D_F/a^2$ vs x . Bottom: Magnetic field components and $j_{||}$ versus x ; each curve is normalized to 1 at $x=0$.

C. Example of slab-model force-free state with tapered magnetic diffusivity

Laboratory force-free configurations [e.g., RFP (Ref. 6) and spheromak⁷ experiments] are generally encased in a metallic, rigid conducting wall. Time-varying magnetic fields (\tilde{B}_z) normal to and in the vicinity of the wall are systematically reduced in amplitude by eddy currents in the wall, relative to the \tilde{B}_r amplitudes that would occur in the absence of such a wall. This should lead to a systematic reduction in the magnetic diffusivity near the plasma boundary, because² $D_F \sim B_r^2/B^2$.

We now include this effect in our slab model by letting $D_F(x)$ vary as shown in Fig. 7 (top). The diffusivity drops by a factor of 25 over a narrow transition region ($\Delta x/a \approx 0.2$) centered at $x/a = 0.6$. We continue to require the plasma to be isothermal all the way to $x=a$, however, and continue to use an insulating boundary condition at the wall: $\partial f^{(1)}(\vec{v}, x)/\partial x \rightarrow 0$ as $x \rightarrow a$. The core diffusivity coincides with the uniform diffusivity [$\lambda_0 D_F(0)/a^2 = 0.05$] used in Fig. 2. The magnetic fields and current-density profiles for the tapered diffusivity case are shown in Fig. 7 (bottom). In contrast to Fig. 2, the $j(x)$ profile in Fig. 7 drops more precipitously in the edge ($x/a \gtrsim 0.7$).

D. Discussion

We have shown that strongly sheared magnetoplasmas with sufficiently large magnetic field diffusivity and elec-

tron scattering length can be explained on the basis of nonlocal electrical conductivity. In these circumstances a local Ohm's law is obviously incorrect: The ratio of time-averaged $j_{||}(x)$ over time-averaged $E_{||}(x)$ will *not* be a spatial constant (in our isothermal model) equal to σ_L . Nonetheless, the notion of conductivity has proved convenient elsewhere for estimating a plasma discharge's "temperature" by external electrical measurements,¹² which are far easier than, e.g., Thomson scattering measurements of the electron distribution function. Thus it would be useful to utilize the conductivity parameter σ by defining it in terms of spatial integrals over the plasma,¹² instead of a local constitutive relation.

To do this, let us multiply both sides of Eq. (11) by $-ev \cos\theta$ and then integrate over both \vec{v} and x . Then the boundary condition ($\partial f^{(1)}/\partial x = 0$ at $x=0, a$) causes the diffusion term in Eq. (11) to integrate to 0, and we obtain

$$\langle j_{||} \rangle = \sigma_L \langle E_{||} \rangle, \quad (19)$$

where $\langle \rangle$ means spatial average. This formally resembles an Ohm's law and, more significantly, the "conductivity" is precisely that of the nominal local Ohm's law. The global Ohm's law [Eq. (19)] is based on global *momentum* balance between acceleration and scattering. We emphasize that Eq. (11) *cannot* be integrated (except in the trivial case where $\partial E_{||}/\partial x = 0$) to give a global Ohm's law based on dissipation *that has the nominal local conductivity*. That is,

$$\langle j_{||}^2 \rangle \neq \sigma_L \langle j_{||} E_{||} \rangle. \quad (20)$$

This comparison of momentum- and dissipation-based definitions of global conductivity leads to a conclusion already reached elsewhere¹² in the context of a $\vec{v} \times \vec{B}$ dynamo and magnetic helicity dissipation. The conclusion of Ref. 12 is found to apply equally well to our momentum-diffusion model as to the dynamo.

Our slab-model solutions tend toward $j_{||} \rightarrow \text{const}$ in the limit $\lambda_0 D_F/a^2 \rightarrow \infty$. Our kinetic equation accomplishes this by allowing electrons to follow field-line trajectories. We plan to treat the generalization of this effect to cylindrical force-free plasmas in a forthcoming publication. At this point we note two properties of the cylindrical case; both are due to the fact that the magnetic field intensity B must vary with r in cylindrical force-free equilibria: First, the tendency $j_{||} \rightarrow \text{const}$ (in the slab case) becomes $j_{||}/B \rightarrow \text{const}$ in the cylinder. This is due to the facts that (a) electrons wander along field lines, and (b) the density of field lines is B . Second, the cylinder differs from the slab in another, and less trivial way, due to the magnetic mirror force on an electron wandering in radius along the gradient $\partial B/\partial r$. This requires that (except for collisions) $\cos\theta$ be replaced by the electron's magnetic moment as a constant of the motion.

Although our nonlocal-conductivity model is steady state, it can provide some insight into the relaxation time required to approach the steady force-free configuration following a sudden change in either D_F or the drive electric field E_z : Because the global $j(x)$ profile is due to electron wander over the gradient of $E_{||}$, the minimum settling time for a $j(x)$ profile is the time required for a typi-

cal current-carrying electron either to sample the gradient length or to scatter, whichever is less.

Finally, the model we have presented differs (apart from geometry) from actual laboratory plasmas in two interrelated ways: First, the model is isothermal, whereas experiments occur next to a necessarily cold boundary and thus must have a temperature gradient. Second, in a real experiment we cannot rule out electron wander all the way to the material wall (balanced by, e.g., secondary emission from the wall). This would enable direct loss of electron momentum to the wall and would further increase the required electric field E_z to sustain a given configuration. This would correspond to a systematically higher "apparent resistivity" than is implied by Fig. 5.

Aspects of our nonlocal-conductivity mechanism have been suggested in earlier publications of other authors. Three publications by Stix have dealt with cross-field electron transport in stochastic magnetic fields: The first two^{13,14} point out that stochasticity will inevitably redistribute force-free currents $j_{||}$, while the third¹⁵ proposes a specific mechanism involving propagation of Alfvén waves following transient magnetic reconnection. Although the specific mechanism¹⁵ of driving nonlocal currents $j_{||}$ does not coincide with our kinetic process, the suggestion that magnetic braiding would give rise to current diffusion is an antecedent to our own work. Another antecedent is in Ref. 3: a suggestion that stochastic wander of electrons will give rise to an effective electron shear viscosity. Although the context of that sug-

gestion³ was plasma microinstabilities, it is an approximate description of the electron-momentum transport in our kinetic mechanism. Finally, a treatment by Speiser¹⁶ of anomalously fast magnetic reconnection in the Earth's magnetotail shows that the apparent resistivity, which determines the diffusion-layer thickness, may be more a product of finite electron storage time (in the layer) than of collisions with particles. This approach is somewhat similar to our treatment of electron-momentum diffusion down the gradient $\partial E_{||}/\partial x$: Electrons carry field-aligned momentum out of the high- $E_{||}$ region before scattering.

Our development has heavily relied on the description in Ref. 3 of electron wander along stochastic magnetic field lines. We remark that similar descriptions have been offered by Stix¹⁵ and by Jokipii and Parker.¹⁷

Our nonlocal-conductivity mechanism may be compared to an earlier model of RFP sustainment, the tangled discharge mechanism (TDM) proposed by Rusbridge¹⁸ and further discussed by Miller.¹⁹ The TDM applies to the regime where the collision length is sufficiently short to ensure a local Ohm's law. In contrast, our mechanism applies to the opposite regime, where the collision length is long enough to void a local Ohm's law.

ACKNOWLEDGMENT

We have benefited from discussions with Ross Spencer and Richard Nebel on the properties of stochastic magnetic fields.

¹L. Spitzer and R. Härm, *Phys. Rev.* **89**, 977 (1953).

²M. N. Rosenbluth, R. Z. Sagdeev, J. B. Taylor, and G. M. Zaslavsky, *Nucl. Fusion* **6**, 297 (1966).

³A. B. Rechester and M. N. Rosenbluth, *Phys. Rev. Lett.* **40**, 38, (1978).

⁴H. Knoepfel and D. A. Spong, *Nucl. Fusion* **19**, 785 (1979).

⁵R. H. Levine, *Solar Phys.* **46**, 159 (1976).

⁶H. Dreicer, *Physica Scripta* **T2/2**, 435 (1982).

⁷D. A. Baker *et al.*, in *Plasma Physics and Controlled Nuclear Fusion Research 1982*, 9th Conf. Proc. [*Nucl. Fusion Suppl.* **1**, 587 (1983)].

⁸E. J. Caramana, D. A. Baker, and R. W. Moses, Los Alamos National Laboratory Document No. LA-UR-83-2284 (1983) (unpublished).

⁹J. B. Taylor, *Phys. Rev. Lett.* **33**, 1139 (1974).

¹⁰C. G. Gimblett and M. W. Watkins, in *Controlled Fusion and Plasma Physics*, proceedings of the Seventh European Conference, Lausanne, 1975 (Centre de Recherches en Physiques des Plasmas, Lausanne, 1975), Vol. 1, p. 103.

¹¹R. J. Bickerton, *Proc. Phys. Soc. London* **72**, 618 (1958).

¹²K. F. Schoenberg, R. W. Moses, and R. L. Hagenson (unpublished).

¹³T. H. Stix, *Phys. Rev. Lett.* **30**, 833 (1973).

¹⁴T. H. Stix, *Phys. Rev. Lett.* **36**, 521 (1976).

¹⁵T. H. Stix, *Nucl. Fusion* **18**, 353 (1978).

¹⁶T. W. Speiser, *Planet. Space Sci.* **18**, 613 (1970).

¹⁷J. R. Jokipii and E. N. Parker, *Astrophys. J.* **155**, 777 (1969).

¹⁸M. G. Rusbridge, *Plasma Phys.* **19**, 499 (1977).

¹⁹G. Miller, Los Alamos National Laboratory Document No. LA-UR-83-2688 (1983).